MONTE CARLO SIMULATION OF FLUORESCENCE CORRELATION SPECTROSCOPY DATA

Peter KOŠOVAN[a1], Filip UHLÍK[a2], Jitka KULDOVÁ[a3], Miroslav ŠTĚPÁNEK[a4], Zuzana LIMPOUCHOVÁ[a5], Karel PROCHÁZKA[a6,*], Aleš BENDA[b1], Jana HUMPOLÍČKOVÁ[b2] and Martin HOF[b3]

[a] *Department of Physical and Macromolecular Chemistry, Faculty of Science, Charles University in Prague, Albertov 6, 12843 Prague 2, Czech Republic; e-mail: [1] kosovan@lynette.natur.cuni.cz, [2] uhlik@sals.natur.cuni.cz, [3] kuldova@natur.cuni.cz, [4] stepanek@natur.cuni.cz, [5] zl@vivien.natur.cuni.cz, [6] prochaz@vivien.natur.cuni.cz*

[b] *J. Heyrovský Institute of Physical Chemistry, Academy of Sciences of the Czech Republic, v.v.i., Dolejškova 5, Prague 8, Czech Republic; e-mail: [1] benda@jh-inst.cas.cz, [2] humpolickova@jh-inst.cas.cz, [3] hof@jh-inst.cas.cz*

Received October 13, 2009
Accepted January 27, 2011
Published online February 23, 2011

We employed the Monte Carlo simulation methodology to emulate the diffusion of fluorescently labeled particles and understand the source of differences between values of diffusion coefficients (and consequently hydrodynamic radii) of fluorescently labeled nanoparticles measured by fluorescence correlation spectroscopy (FCS) and dynamic light scattering (DLS). We used the simulation program developed in our laboratory and studied the diffusion of spherical particles of different sizes, which are labeled on their surface. In this study, we focused on two complicating effects: (i) multiple labeling and (ii) rotational diffusion which affect the fluorescence signal from large particles and hinder the analysis of autocorrelation functions according to simple analytical models. We have shown that the fluorescence fluctuations can be well fitted using the analytical model for small point-like particles, but the obtained parameters deviate in some cases significantly from the real ones. It means that the current data treatment yields apparent values of diffusion coefficients and other parameters only and the interpretation of experimental results for systems of particles with sizes comparable to the size of the active illuminated volume requires great care and precaution.
Keywords: Diffusion coefficient; Dynamic light scattering; Fluorescence spectroscopy; Monte Carlo method; Rotational diffusion; Translational diffusion.

Fluorescence correlation spectroscopy (FCS)[1] is a noninvasive optical method suitable for studying dynamic processes and determining their parameters, such as the rate constants of chemical reactions[2], flow rates[3], kinetics of various aggregation processes[4], and particularly the translational and rotational diffusion of intrinsically fluorescent or fluorescently labeled species

Collect. Czech. Chem. Commun. 2011, Vol. 76, No. 3, pp. 207–222

doi:10.1135/cccc2009526

ranging from small molecules to nanoparticles. It has been widely used in biochemistry and biology[5–9]. Nowadays its use starts to penetrate also in other fields, e.g., in polymer and colloid science[10,11], although its applications to polymers are still limited.

In our studies of polymer self-assembly, we have been using FCS and dynamic light scattering (DLS) for monitoring the size changes of stimuli-responsive polymeric nanoparticles[12–15]. We found that both techniques yield data that compare reasonably well in most cases, but in some systems differ quite significantly. As the studied polymeric nanoparticles are polydisperse in mass and size and both methods yield different averages of measured values, some differences can be easy understood. However, we found that in certain studied systems, the polydispersity itself does not fully explain the differences and other effects have to be taken into account. In this communication, we focus on two complicating effects that influence the evaluation of FCS data which is based, in the simplest case, on the free diffusion of point-like particles.

The principle of the FSC measurement is the following: In a typical experimental set-up, the excitation light passes through a very dilute (typically 10^{-9} M) solution of fluorescent particles and is focused in a very narrow beam. A small active (effective) volume of roughly ellipsoidal shape, from which the signal (fluorescence emission) is detected, contains only a few fluorescent particles. In a current experimental set-up, the spatial profile of the excitation irradiation, $I(\boldsymbol{r})$, can be approximated by the Gaussian function

$$I(\boldsymbol{r}) = I_0 \exp\left(-\frac{x^2 + y^2}{2\omega_1^2} - \frac{z^2}{2\omega_2^2}\right) \qquad (1)$$

where I_0 is the maximum excitation intensity, $\boldsymbol{r} = (x,y,z)$ is the position with respect to the center of the active volume and ω_1 and ω_2 are the half-axes of the ellipsoid which depend on the experimental set-up. The fluorescent molecules undergo a translational diffusion motion, i.e., they enter and leave the active volume and visit places irradiated with different intensity of the excitation beam. This affects the probability of excitation and causes non-negligible fluctuations in the fluorescence intensity.

The time-resolved monitoring and evaluation of the autocorrelation function of the emission intensity fluctuations yield information on the diffusion rate of fluorescent species. However, the experimental measurement is affected by a number of side effects. At first, the intensity of the focused beam is very high which causes considerable photobleaching (mainly

the transition to the triplet state). Hence only a few very stable and resistant fluorophores (rhodamine dyes or BODIPY) can be employed and still an appropriate correction has to be used when evaluating the diffusion coefficients. At second, the rotational diffusion and multiple labeling of particles of finite size can generate additional problems.

The quantity measured in FCS experiments is the autocorrelation function of the fluorescence intensity fluctuations, $G(\tau)$, defined as

$$G(\tau) = \frac{\langle F(t)F(t+\tau)\rangle}{\langle F(t)\rangle^2} \tag{2}$$

where $F(t)$ is the emission intensity at time t and τ is the lag time. The experimental autocorrelation curves for a system of M types of fluorescent particles (e.g., free probe and several types of labeled nanoparticles characterized by diffusion times $\tau_{D,i}$, absorption cross-sections σ_i and fluorescence quantum yields q_i) can be fitted to the function[14]

$$G(\tau) = 1 + \frac{1 - \Phi(1 - \mathrm{e}^{-\tau/\tau_C})}{\langle N\rangle(1-\Phi)} \times$$

$$\times \sum_{i=1}^{M} Y_i \sigma_i^2 q_i^2 \left(1 + \frac{\tau}{\tau_{D,i}}\right)^{-1} \left[1 + \left(\frac{\omega_1}{\omega_2}\right)^2 \frac{\tau}{\tau_{D,i}}\right]^{-1/2} \tag{3}$$

where $\langle N\rangle$ is the particle number, Φ is the fraction of molecules converted to the triplet state, τ_C is the characteristic time for the transition to the triplet state (τ_C^{-1} is the steady-state transition rate), Y_i are the molar fractions of individual types of particles and ω_1/ω_2 has the same meaning as in Eq. (*1*). It is necessary to point out that the simple model assumes only the translational diffusive motion of point-like particles and does not account for photon correlations caused by rotational motion of large particles which cannot be considered as point-like. If we assume a strictly diffusive motion of photophysically and photochemically stable, chemically uniform and monodisperse point-like particles exited by an exactly Gaussian intensity profile only, Eq. (*3*) simplifies to the form

$$G(\tau) = 1 + \frac{1}{V_{\mathrm{eff}} c_F} \left(1 + \frac{\tau}{\tau_D}\right)^{-1} \left[1 + \left(\frac{\omega_1}{\omega_2}\right)^2 \frac{\tau}{\tau_D}\right]^{-1/2} \tag{4}$$

where we have expressed the particle number as a product of the active (effective) volume, V_{eff} and the average concentration of fluorescent particles, c_{F} (i.e., by their macroscopic concentration neglecting potential "optical tweezer" effect of the strong electric field). The characteristic diffusion time, τ_{D}, is a typical time in which the particle diffuses over the diameter of the active volume. It is related to the translational diffusion coefficient $D = \omega_1^2/4\tau_{\text{D}}$. The ω_1 and ω_2 values and consequently the active volume, V_{eff}, which is theoretically defined as

$$V_{\text{eff}} = \frac{\left[\int_V I(\boldsymbol{r})\mathrm{d}^3\boldsymbol{r}\right]^2}{\int_V I^2(\boldsymbol{r})\mathrm{d}^3\boldsymbol{r}} \tag{5}$$

are in fact adjustable parameters of the optical set-up and can be determined independently by measurements with a small fluorophore with a known diffusion coefficient (e.g., rhodamine B). Thus only two unknown parameters, i.e., c_{F} and τ_{D}, remain to be obtained from the experimental data fit.

With respect to the use of FCS in polymer science, it is instructive to compare the advantages and disadvantages of FCS with the DLS method, which serves as a "benchmark" technique for measuring diffusion coefficients of polymers, nanoparticles and colloidal particles in general. When studying sufficiently large and strongly scattering objects, DLS is a generally applicable technique, which does not require the emission from studied particles and yields more precise data than FCS because it is less affected by parasite side effects. Further it requires the evaluation of a lower number of unknown parameters and the form of the autocorrelation function (exponential time-dependence) facilitates the treatment of polydisperse systems and the separation of the translational diffusion from internal motions by means of an inverse Laplace transformation. Last but not least, the possibility to perform angular measurements provides an additional piece of information on the character of processes that generate fluctuations in the scattered light intensity.

In contrast to the light scattering technique, FCS can be used for a wider range of particle sizes, but it requires strong fluorescence emission of studied species. This apparent drawback is often advantageous and FCS can be used for studying relatively small fluorescent particles in excess of strongly scattering large particles. A thoughtout design of the FCS experiment (pro-

per choice of the extrinsic probe, exploitation of the dependence of the quantum yield on experimental conditions, etc.) can add other advantages[9].

As already mentioned, there is one more significant difference between DLS and FCS results. In dilute solutions of polydisperse or partially aggregating nanoparticles, both techniques yield differently averaged values of the diffusion coefficient: DLS provides the z-average D_z and FLC the number average D_n, defined as

$$D_z = (\Sigma N_i M_i^2 D_i)/(\Sigma N_i M_i^2) \quad \text{and} \quad D_n = (\Sigma N_i D_i)/(\Sigma N_i) \,. \tag{6}$$

The fractions $f_n(M_i) = N_i/(\Sigma N_i)$, $f_w(M_i) = N_i M_i/(\Sigma N_i M_i)$ and $f_z(M_i) = N_i M_i^2/(\Sigma N_i M_i^2)$ are the number, mass (weight) and z-distribution functions of molar masses, M_i of individual particles in a polydisperse sample and D_i are diffusion coefficients of particles with given M_i. The term z-average reflects the fact that the z-average molar masses are determined by analytical ultracentrifugation ("zentrifugation" in German language).

The z-average D_z is strongly affected by the presence of small amounts of large and strongly scattering species, such as microgels, micellar aggregates, which may be a nuisance from the experimental point of view. In some cases the scattering due to traces of strong scatters dominates the signal and information on 90–95 wt. % of the polymer material of interest can be lost. In contrast to light scattering, FCS provides the number average characteristics, which are weighted only by number fractions of particles of different sizes. Further in semidilute solutions, FCS yields the self-diffusion coefficient, while DLS measures the collective diffusion coefficient[16].

In most experimental and theoretical papers devoted to FCS, the studied fluorescent particles were relatively small and the fluorescence fluctuations could have been treated as those caused by the behavior of point-like light emitters. Nevertheless, the application of FCS to nanoparticles is not straightforward because there exist a number of inherent problems connecting with the behavior of large fluorescent particles on the molecular level that affect the autocorrelation function and have to be taken into account. The role of complicating factors, such as internal flexibility of fluorescently labeled species, their finite size, multiple labeling, overall rotation or internal rotation of their parts, etc., has been only little studied and some of them have never been taken into account. Therefore their effect on the measured characteristics, possible mutual compensation, etc. is almost unknown.

In this paper, we focus on two complicating effects arising in systems of nanoparticles of a non-negligible size (e.g., polymeric micelles, vesicles),

which carry several fluorescent labels. First we study the effect of size of diffusing fluorescent nanoparticles on the parameters obtained from the fit of the autocorrelation function. When the dimensions of such particles are comparable to those of the effective volume (ω_1, ω_2), the correlated motion of fluorophores located on the same particle affects the shape of the autocorrelation function. Recently, an approximate expression for the FCS autocorrelation function for multiply labeled diffusing particles of finite size has been derived by Wu et al.[17] It has been shown that it can be expressed in the form similar to Eq. (*3*) where the diffusion time, concentration and dimensions of the active volume are replaced by corresponding apparent quantities depending on the relative particle size. In this paper, we test the theoretical prediction by computer simulation. In the second part, we study the effect that has not yet been addressed in the literature. It concerns the contribution to the autocorrelation function, which cannot be neglected for large particles and which stems from their rotational motion. Even though this problem has not been treated theoretically so far, one can intuitively expect that when a large particle rotates, the mean-square displacement of embedded flurophores should be larger than that without the rotation. In such a case, should FCS yield a higher apparent diffusion coefficient than that for the pure translational diffusion. In this paper, we address the two above described complicating effects by computer simulations.

MONTE CARLO SIMULATION OF FCS DATA

We use a simple simulation program, which has been developed in our laboratory. It emulates the behavior of an ensemble of fluorescently labeled particles diffusing in a volume irradiated by a laser beam with defined spatial intensity profile. The particles can be either point-like or monodisperse (characterized by one value of D) finite-size (effectively spherical, i.e. from the rotational point of view, reasonably described by one parameter only) and they perform both the translational and rotational diffusive motion. Because the exact solution of the translation diffusion (free of any simplifying assumptions) exists, the probability of displacement in time interval Δt can be drawn directly from the known probability distribution (without applying any acceptance criterion)

$$P(x,\Delta t) = \frac{1}{2}\sqrt{\pi D\Delta t}\exp\left(-\frac{x^2}{4D\Delta t}\right) \qquad (7)$$

where x is the position of the particle and D is the translational diffusion coefficient. Besides the translational diffusive motion, the finite-sized objects perform also the rotational diffusion. The rotational diffusion is simulated "from definition" (because there exists no appropriate analytical expression), i.e., in the time interval Δt, each object is rotated n_{rot} times (n_{rot} = 10 is sufficient) around random axes by an angle ϕ given by the expression

$$\varphi = \sqrt{\frac{6\Theta\Delta t}{n_{\mathrm{rot}}}} \tag{8}$$

where Θ is the rotational diffusion coefficient which is related to the translational diffusion coefficient, D, as

$$\Theta = \frac{kT}{8\pi\eta R^3} = \frac{3D}{4R^2} \tag{9}$$

where R is the radius of the particle, k is the Boltzmann constant, T is the temperature and η is the viscosity of the solvent. Each of the diffusing particles can carry several fluorescent labels distributed either in its volume or at the surface. The number of emitted photons in the interval Δt obeys the Poisson distribution

$$P_\nu(n) = \nu^n \frac{\mathrm{e}^{-\nu}}{n!} \tag{10}$$

where ν is the expected mean number of photon emissions. For a particle in position (x,y,z), ν can be expressed as

$$\nu = Q\,\Delta t I(x,y,z) \tag{11}$$

where $I(x,y,z)$ is the excitation profile defined by Eq. (*1*) and Q is the apparatus constant. In a real system Q comprises a number of factors such as detection efficiency and quantum yield. In the simulation it is an adjustable parameter, which has no effect on the results, but influences the computational efficiency. The size of the spherical simulation cell exceeds sufficiently the size of the effective volume, which is located in its center. We apply spherical boundary conditions: when a particle diffuses out of the simulation cell, it is deleted and a new particle is generated at a random position on the surface of the cell. The boundary conditions perturb the corre-

lations at longer times, which may cause potential problems, i.e., it can slightly distort the correlation function and cause a certain error in the diffusion correlation time estimation. The error can be suppressed by increasing the size of the simulation box and prolonging the simulation run. The presented correlation is a compromise between the accuracy and computer time. For practical purposes, we accept an error ca. 5% in both the diffusion coefficient and concentration (estimated from a series of simulations differing in the size of the simulation box and the simulation time), which is better than the experimental accuracy.

RESULTS AND DISCUSSION

Experimental Data

For almost one decade, we have been using both DLS and FCS for studying the self-assembling polymer systems. In a few of our recent papers[13–15] we used octadecyl rhodamine B (ORB; Fig. 1) as a fluorescent marker. ORB is suitable for labeling the micelles because it is an amphiphilic fluorophore very little soluble in water which binds very strongly to polymeric core-shell nanoparticles. Moreover, it has very low intersystem-crossing rate,

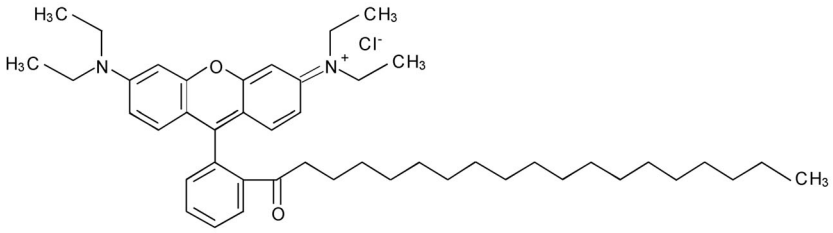

FIG. 1
Octadecyl rhodamine B

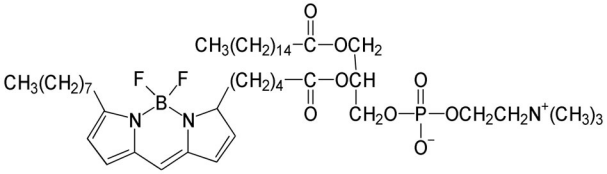

FIG. 2
BODIPY phopholipid derivative

which makes it highly resistant to photobleaching and as the free ORB forms self-quenched aggregates in aqueous media, the contribution of the free probe emission to the signal is very low. In this study, we use one more dye, BODIPY phospholipid derivative (Fig. 2) which is also very photoresistant and strongly binds to nanoparticles.

As already mentioned, in the studied polymer systems, which are always non-negligibly polydisperese and contain particles which differ in molar mass and size, several different averages of all properties depending on molar mass and size, can be defined and measured by different experimental techniques. As concerns molar masses in particular, the number average, mass (weight) average and z-average molar masses, M_n, M_w and M_z, respectively,

$$M_n = (\Sigma N_i M_i)(\Sigma N_i),\ M_w = (\Sigma N_i M_i^2)/(\Sigma N_i M_i) \text{ and } M_z = (\Sigma N_i M_i^3)/(\Sigma N_i M_i^2) \quad (12)$$

can be obtained by osmotic pressure, static light scattering and centrifugation measurements[18]. While M_w and M_z are usually measured with a sufficient accuracy by the above mentioned benchmark techniques, the osmotic pressure of high-molar-mass polymer solutions is very low (at a given weight concentration, the number of long chains is very low) and the measured molar masses are subject of large experimental errors. In our studies of fluorescently labeled polymeric nanoparticles, we addressed the problem of an accurate estimation of M_n and developed a simple titration method for a relatively precise evaluation of the number-average molar mass, M_n of amphiphilic water-soluble nanoparticles. In our FCS method, an aqueous solution of the fluorescent surfactant with a strong affinity to polymeric nanoparticles and the self-quenched fluorescence (due to the formation of associates) is continuously added to the aqueous solution of nanoparticles. At relatively low fluorophore-to-nanoparticle ratios, ξ, single fluorophore molecules (which are no more self-quenched) bind to different nanoparticles and the fraction of labeled fluorescent particles increases, which means that the particle number, $\langle N \rangle$, measured as the frequency of fluctuations, grows. When $\xi = 1$, each nanoparticle is on average labeled by one fluorescent probe (in reality, there exists the Poisson distribution of the number of probes per one micelle) and the added probes start to bind to the already labeled polymer particles. If the size of nanoparticles is small enough, the frequency of fluctuations stops to increase and levels off, because the detector registers the double-labeled (or multiply-labeled) particle as one "point". The only difference is that some fluctuations are significantly larger than the others. The experimental frequency as a function of

the added amount of the probe consists of a linearly increasing and a constant part. The crossing point yields the number concentration of nanoparticles and the number-average molar mass. Typical data for micelles are shown in Fig. 3. Here we show data for micelles formed by PS_{136}-PVP_{117}-PEO_{795} copolymer studied in detail in ref.[17]. Evaluation of FCS titration curve yields the molar mass $\langle M \rangle_n = 0.5 \times 10^6$ g mol^{-1} and static light scattering measurement gives $\langle M \rangle_w = 2.7 \times 10^6$ g mol^{-1}.

The fits of the FCS and DLS autocorrelation curves yield the z- and n-average diffusion coefficients that can be recalculated in appropriately weighted hydrodynamic radii using the Stokes–Einstein formula, $R_H = kT/(6\pi D\eta)$, where k is Boltzmann constant, T temperature and η viscosity of the solvent (R_H represents the radius of a hard sphere which has the same hydrodynamic properties as the studied (roughly spherical) object and is called either the hydrodynamic radius, or more precisely the radius of a hydrodynamic equivalent sphere). The pertinent values are $\langle R_H^{-1} \rangle_n^{-1}$ = 28 nm and $\langle R_H^{-1} \rangle_z^{-1}$ = 37 nm. The observed differences are in this particular case of relatively small particles caused by a non-negligible polydispersity.

Fairly soon we observed that the developed method gives good and reliable results for relatively small nanoparticles (R_H ca. 10–30 nm, M_n ca. 10^5–10^7 g mol^{-1}), but it strongly underestimates molar masses of large nanoparticles (R_H higher than 50 nm). We observed some smaller devia-

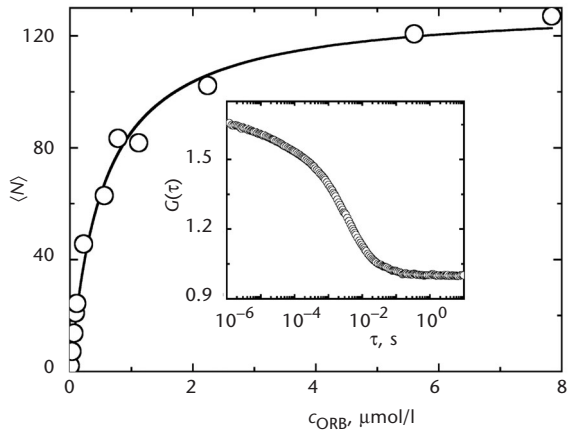

FIG. 3
Particle number $\langle N \rangle$ as a function of the fluorescent probe concentration c_{ORB} for PS-PVP-PEO micelles in 0.01 M HCl. Insert: Typical correlation curve for an FCS measurement of ORB-labeled PS-PVP-PEO micelles in 0.01 M HCl

tions also for R_H higher than 30 nm, depending on the system studied. As the M_n evaluation is very simple and does not require fitting the correlation curve, the analysis of discrepancies is straightforward and shows that the multiple labeling of large particles causes higher frequency of fluctuations than it would correspond to the correct particle number, because two spatially separated labels at one particle are registered as two time-separated fluctuations. A careful comparison of results of both methods (based on autocorrelation functions) shows that FCS always yields lower values (both molar masses and hydrodynamic radii) than the light scattering. Table I gives several typical examples. As already explained, the differences are due, in part, to different weighting, but also to the finite size effect and multiple labeling. In the next part, we will analyse the effects of the two latter-mentioned complicating factors.

All FCS measurements presented in this communication were performed with a ConfoCor I binocular microscope (Carl Zeiss, Germany) equipped with a 514 nm argon laser, an adjustable pinhole together with a special fluorescence optics, SPCM-200PQ detection diode and an ALV-5000 correlator (ALV, Langen, Germany). The preparation of micelle-like nanoparticles (labeled by ORB for FCS measurements) has been described in references listed in Table I. 1,2-Dioleoyl-sn-glycero-3-phosphocholine (DOPC) vesicles (for results see later in Fig. 4) were prepared by a standard extruder method[19] and labeled by a BODIPY phospholipid derivative (Fig. 2). The fluorescent probes were purchased from Molecular Probes, Ltd., USA.

TABLE I
Molar masses and hydrodynamic radii of several micellar systems, measured by light scattering and by FCS

Copolymer[a] solvent	$\langle M\rangle_w \times 10^{-6}$ g mol^{-1}[b]	$\langle M\rangle_n \times 10^{-6}$ g mol^{-1}[c]	$\langle R_H^{-1}\rangle_z^{-1}$ nm[b]	$\langle R_H^{-1}\rangle_n^{-1}$ nm[c]	Reference
PS_{198}-PMA_{221} 0.05 M $Na_2B_4O_7$	8.0	4.7	54	42	13
PS_{136}-PVP_{117}-PEO_{795} 0.01 M HCl	2.7	0.5	37	28	14
PS_{136}-PVP_{117}-PEO_{795} 0.01 M NaOH	5.4	1.1	35	22	14
PS_{29}-PVP_{117}[d] 0.1 M HCl	0.8	0.5	32	28	15

[a] Subscripts denote degrees of polymerization of the blocks. [b] Measured by LS. [c] Measured by FCS. [d] Multiarm star copolymer with 20 PS_{29} and 20 PVP_{217} arms.

Results of Simulations

Before we analyse the effects of the finite size and multiple labeling of studied particles, we will demonstrate that the simulation of FCS curves for thepoint-like particles, i.e., that based on the translational diffusion only, reproduces experimental data for relatively small and scarcely labeled polymeric nanoparticles reasonably well and provides correct size characteristics. Figure 4 shows a comparison of experimental and simulated FCS autocorrelation functions. The experimental autocorrelation function (open squares) for 1,2-dioleoyl-sn-glycero-3-phosphocholine (DOPC) vesicles weakly labeled by BODIPY phospholipid derivative has been corrected for the transition to the triplet state (using values Φ and τ_C obtained from the fit and subtracting the second term in Eq. (*3*)) to get the neat effect of the diffusion. The vesicles were characterized both by DLS and FCS. As the z- and n-based reciprocal values of hydrodynamic radii, obtained from fits of pertinent autocorrelation functions, $(R_H^{-1})_z^{-1}$ = 30.2 ± 0.2 nm and $(R_H^{-1})_n^{-1}$ = 27.7 ± 0.5 nm, respectively, differ only little, the system seems to be reasonably monodisperse in size. The curve is the simulated autocorrelation curve for the same $(R_H^{-1})_n^{-1}$ and parameters of the optical set-up as in the experiment. It is obvious that both curves are almost identical which, e.g., proves that the developed simulation program works correctly and the computer modelling reproduces the behavior of studied fluorescent particles well.

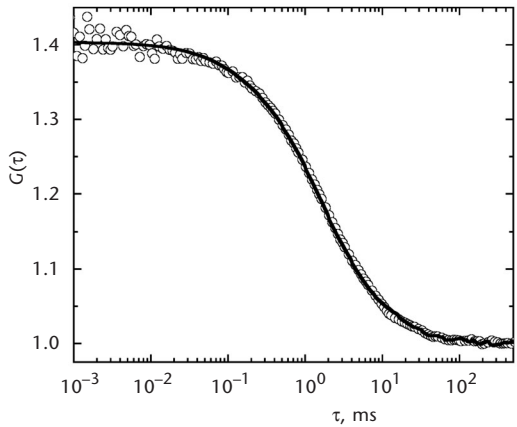

FIG. 4
The comparison of the experimental FCS autocorrelation function due to diffusion only, i.e., that corrected for the transition to the triplet state (□) with the MC simulated data (——)

A certain, unfortunately hidden, problem consists in the fact that for large particles, the experimental and simply simulated curves (i.e., without taking the rotational diffusion into account) coincide also very well (not shown), but the size evaluated from the fit is evidently unrealistic.

In the next part, we use the computer simulations to study the effect of the size of diffusing particles and the number of labels on the results obtained by FCS measurements. The simulated particles are spheres and can carry one or more fluorophores on their surface. The translational diffusion coefficient of particles (describing the motion of their centers of gravity) was calculated from Eq. (*9*) and used as an input parameter. The fluctuating fluorescence intensity of the simulated system was processed to calculate the autocorrelation function $G(\tau)$ (Eq. (*2*)) which was then fitted using the analytical expression for point-like particles (Eq. (*4*)).

In the first series of simulations, we neglect the rotational diffusion and study only the effect of the size and multiple labeling. We performed a series of simulations for increasing number of labels. Here we present only selected data for one and four labels as typical examples which demonstrate the trends of the behavior fairly well. The open circles (curve *2*) in Fig. 5a show the simulation data for particles carrying one label only. The vertical axis shows the ratio of the apparent diffusion time (i.e., that obtained from the fit of the simulated autocorrelation function) to the true diffusion time (input parameter of the simulation). The horizontal axis gives the ratio of the particle radius, R, and the typical dimension of the active volume, ω_1. The theory predicts that the particles carrying only one label behave as the

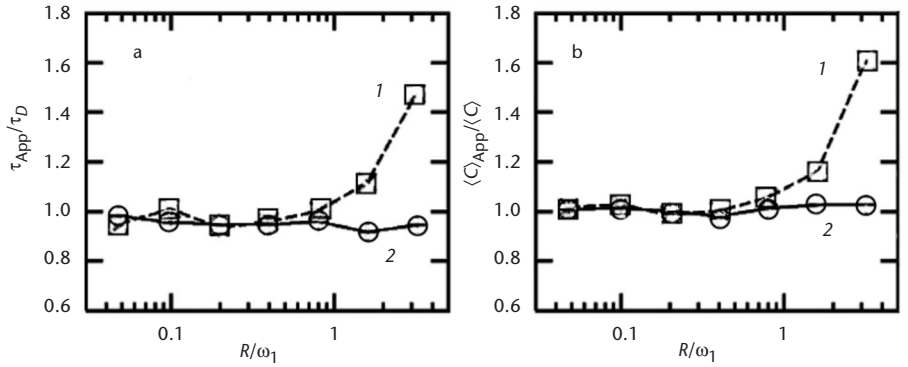

FIG. 5
The apparent diffusion time τ_{App} (a) and concentration $\langle C\rangle_{App}$ (b) as functions of the particle radius R: four labels (*1*) and one label (*2*) per particle

point-like particles and the diffusion of the labels (monitored by FCS) corresponds exactly to that of their centers of gravity. Therefore we should obtain the ratio $\tau_{App}/\tau_D = 1.0$. The deviations characterize intrinsic error of the simulation (up to 5% – predetermined precision of simulation). The simulation and theoretical data agree well and we use the simulation data for single labeled particles as a reference data set for comparison with other results. If the particles carry more fluorescent labels, the motions of labels attached to the same particle are correlated which affects the autocorrelation function. In this case, the data fitting according to Eq. (*4*) yield an apparent diffusion time, which could differ significantly from that describing the particle gravity center motion. In Fig. 5a, the open squares (curve *1*) show the simulation results for particles carrying 4 labels. The apparent diffusion time does not significantly differ from the true value for $R << \omega_1$. However, it increases and differs significantly from the real value when $R \approx \omega_1$. This observation compares well with the theoretical predictions by Wu et al.[17]. A similar plot for the apparent concentration is shown in Fig. 5b. Again, for small point-like particles, the open circles (curve *2*) are very close to unity for any particle size while the open squares (4 labels) deviate significantly from the real ones when $R \approx \omega_1$.

Another unexplored problem is the role of the rotational diffusion of particles in FCS studies. Intuitively, the rotational diffusion is expected to speed up the decay of the autocorrelation function. Therefore one should presumably observe a shorter apparent diffusion time. This hypothesis was confirmed by a series of simulations. The obtained data are shown in Fig. 6a. The reference curve *2* is the same as in Fig. 5a. The open squares

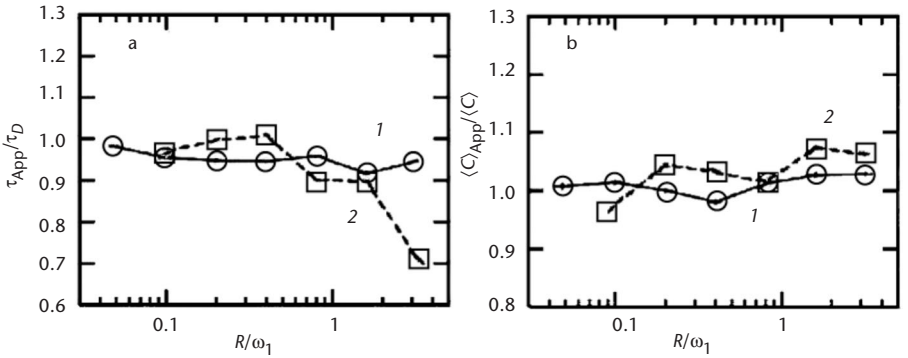

FIG. 6
The apparent diffusion time τ_{App} (a) and concentration $\langle C\rangle_{App}$ (b) as functions of the particle radius R: for non-rotating (*1*) and rotating (*2*) particles

show the system, which undergoes the rotational diffusion. As expected, when the relative size of the particle is small in comparison with the dimensions of the active volume, the rotation has only little effect, but when the particle dimensions become comparable to those of the active volume, the apparent diffusion time decreases. When the multiply labeled particles undergo the rotational diffusion (data not shown), the effect of rotation is suppressed. It can be understood by analysing the extreme case: in the limit of very high number of labels, the large particle is uniformly covered with fluorophores and it does not matter at all if it is rotating or not. Hence, with increasing number of fluorescent labels on the studied particle, the effect of rotation gradually diminishes. Fig. 5b shows that the apparent concentration is only little affected by the rotation (the observed differences are close to the intrinsic error of the method and hence can be considered as negligible).

CONCLUSIONS

To summarize the obtained results of Monte Carlo (MC) simulations and compare the effects of studied complicating factors with those observed in experimental studies, we can say that the autocorrelation curves can be in all cases fitted well by functions (and simulated well by computer-based MC methods) that take into account the translational diffusion only, but the apparent parameters obtained from the fits for large particles are obviously unrealistic, while those for small particles are reasonable. The computer simulations show that the number of labels (and their distribution) significantly affects the FCS autocorrelation function when the size of multiply labeled particles, is comparable with the effective illuminated volume. If such particles undergo the translational diffusion only, the total motion of probes reflects not only the diffusion motion of whole particles, but also a mutually correlated motion of several probes at one particle. If such systems are treated using the standard model for the point-like particles, the obtained apparent diffusion times are longer and differ significantly from the real ones. However, if a large particle undergoes also the rotational diffusive motion, then the apparent diffusion time decreases. Hence for large particles, both effects cause deviations in opposite directions and may partially compensate each other. The effect of the rotational diffusion is important when there is only one label per particle and diminishes with increasing number of labels. Both effects should be taken into account when FCS data on particles with non-negligible dimensions are treated and interpreted. On a semi-qualitative basis, the above-presented results of simula-

tions explain some discrepancy between the diffusion coefficients (hydrodynamic radii) of large particles measured by FCS and DLS. The simulation results concerning the multiple labeling of finite size particles also confirm our interpretation of measurements of M_n of multiply labeled particles of non-negligible size. When the size of multiply labeled particles increases (Fig. 4b), the particle number (i.e., total rate of fluctuations) also increases, which leads to a decrease in the measured M_n.

The authors are grateful for the support by the Ministry of Education, Youths and Sports of the Czech Republic (Research Plan MSM0021620857 and Czech-German Grant MEB 100907), Czech Science Foundation (Grant No. 203/07/0659) and Grant Agency of the Academy of Sciences of the Czech Republic (Grants IAA400500703, IAA401110702 and IAA400400621).

REFERENCES

1. Magde D., Elson E. L., Webb W. W.: *Biopolymers* **1974**, *13*, 29.
2. Aragón S. R., Pecora R.: *J. Chem. Phys.* **1976**, *64*, 1791.
3. Asai H.: *Jpn. J. Appl. Phys.* **1980**, *19*, 2279.
4. Peterson O. N.: *Biophys J.* **1981**, *33*, 435.
5. Schwille P., Bieschke J., Oehlenschlager F.: *Biophys. Chem.* **1997**, *66*, 211.
6. Schwille P.: *Cell Biochem. Biophys.* **2001**, *34*, 383.
7. Sanchez S. A., Gratton E.: *Acc. Chem. Res.* **2005**, *38*, 469.
8. Remaut K., Lucas B., Raemdonck K., Beckmans K., Demeester J., De Smedt S. C.: *J. Controlled Release* **2007**, *121*, 49.
9. Humpolíčková J., Beranová L., Štěpánek M., Benda A., Procházka K., Hof M.: *J. Phys. Chem. B* **2008**, *112*, 16823.
10. Zettl H., Hafner W., Boker A., Schmalz H., Lanzendorfer M., Müller A. H. E., Krausch G.: *Macromolecules* **2004**, *37*, 1917.
11. Bonne T. B., Papadakis C. M., Ludtke K., Jordan R.: *Colloid Polym. Sci.* **2006**, *285*, 491.
12. Humpolíčková J., Procházka K., Hof M., Tuzar Z., Špírková M.: *Langmuir* **2003**, *19*, 4111.
13. Matějíček P., Podhájecká K., Humpolíčková J., Uhlík F., Jelínek K., Limpouchová Z., Procházka K., Špírková M.: *Macromolecules* **2004**, *37*, 10141.
14. Štěpánek M., Humpolíčková J., Procházka K., Hof M., Tuzar Z., Špírková M., Wolff T.: *Collect. Czech. Chem. Commun.* **2003**, *68*, 2120.
15. Štěpánek M., Matějíček P., Humpolíčková J., Havránková J., Podhajecká K., Špírková M., Tuzar Z., Tsitsilianis C., Procházka K.: *Polymer* **2005**, *46*, 10493.
16. Zettl U., Hoffmann S. T., Koberling F., Krausch G., Enderlein J., Harnau L., Ballauff M.: *Macromolecules* **2009**, *42*, 9537.
17. Wu B., Chen Y., Muller J. D.: *Biophys. J.* **2008**, *94*, 2800.
18. Munk P.: *Introduction to Macromolecular Science*. Wiley, New York 1989.
19. Hutterer R., Schneider F. W., Sprinz H., Hof M.: *Biophys. Chem.* **1996**, *61*, 151.